CrossMark

# Synthesis of L-Cysteine Capped Silver Nanoparticles in Acidic Media at Room Temperature and Detailed Characterization

Sallahuddin Panhwar[1] · Syeda Sara Hassan[1] · Rasool Bux Mahar[1] · Ali Canlier[2,3] · Sirajuddin[4] · Munazza Arain[5]

## Abstract

This work reports a simple and one pot synthesis of water dispersible L-cysteine stabilized silver nanoparticles (L-CYS-AgNPs) in an acidic media. Silver nanoparticles were synthesized within few minutes of reaction time (< 5 min) at room temperature without needing to heat and use of any hazardous organic solvents. Prepared nanoparticles were characterized by UV–Visible spectroscopy, Fourier transform infrared spectroscopy, transmission electron microscopy, atomic force microscopy, X-ray diffraction and zeta potential analysis, respectively. Surface plasmon resonance band of AgNPs which was observed at 392 nm by UV–Visible spectroscopy indicated successful formation of L-CYS-AgNPs in acidic media. Imaging techniques showed that AgNPs possess spherical morphology and average size of 25 nm. Nanoparticles were stable for more than 2 months when stored at ambient temperature. This approach is a facile and rapid one pot synthesis which can be stored as a homogenous aqueous dispersion for more than 2 months. Being stabilized by a sulfur-containing amino acid (L-cysteine) and the synthesis carried out in a moderately acidic media (pH 5.3) are distinctive aspect of this work. These stable L-CYS-AgNPs could be used as a catalyst and sensor applications for advanced perspective against water pollution and industrial effluents.

**Keywords** Nanoparticles · Silver · L-Cysteine · Acidic media · Water dispersible

✉ Sallahuddin Panhwar
  panhwarsallahuddin@yahoo.com

✉ Syeda Sara Hassan
  ssarahassan@gmail.com

1. U.S.-Pakistan Center for Advanced Studies in Water (USPCAS-W), Mehran University of Engineering & Technology (MUET), Jamshoro 76062, Sindh, Pakistan

2. Department of Chemical Engineering and Applied Chemistry, College of Engineering, Chungnam National University, Daejeon 34134, South Korea

3. Department of Materials Science and Nanotechnology Engineering, Abdullah Gul University, 38080 Kayseri, Turkey

4. National Center of Excellence in Analytical Chemistry, University of Sindh, Jamshoro 76082, Sindh, Pakistan

5. Dr. M. A. Kazi Institute of Chemistry, University of Sindh, Jamshoro, Sindh, Pakistan

## 1 Introduction

Nanoparticles with a size between 1 and 100 nm, which have attracted considerable attention from researchers due to their unique properties [1] in various fields and applications such as catalysis [2, 3], molecular recognition [4], antibacterial activity [5] and sensing [6]. Nanoparticles of particularly silver (Ag), gold (Au) and copper (Au) metals are drawing more attention than other metal nanoparticles due to their fascinating and unique properties such as exhibiting localized surface plasmon resonance (LSPR) [7]. Among these metal nanoparticles, AgNPs possess excellent electrical and thermal conductivity adding to a large surface area to volume ration altogether enabling outstanding catalytic activity and nonlinear behavior of Raman scattering [8–10]. Physically homogenous synthesis of nanoparticles is the main challenge in order for gaining unvarying chemical composition, size distribution, morphology, and crystal structure. For synthesis of AgNPs, there are various synthesis procedures which are reported [11, 12]. In each and every method have some advantages and disadvantages such as cost, scalability, particle size and shape distribution in physical, chemical and

biological routes. Amongst available techniques, chemical method is the most commonly used process for the synthesis of AgNPs because it offers an easy way to synthesize AgNPs in solution environment. Such chemical synthesis process of silver nanoparticles characteristically and usually includes use of metal precursors, reducing and capping agents [13, 14]. Size, geometry and optical property yield of dispersed silver nanoparticles are providing excellent applications in biological assays as well [15]. Most researchers suggest that spherical geometry of nanoparticles is suitable for most practical applications with their colloidal form [16, 17]. In most cases synthesis of AgNPs result in a range of particle sizes, and forms which suggest stringent limits to controlling size, geometry and stability of dispersion in solution [18]. On the other hand, few illustrations using immediate reduction ability of $NaBH_4$ agent yielded highly dispersible and near-uniform AgNPs [17]. $NaBH_4$ is a desired agent with its strong reducing ability for formation of uniformly sized and dispersed silver nanoparticle colloids as well as achieving smaller size of nanoparticles [19, 20]. In AgNPs synthesis process, stability of nanoparticles plays a vital role for further applications thus various capping and stabilizer agents are resorted to increase the dispersion stability [21]. Numerous studies reported that synthesis of naked AgNPs in colloidal state though stability and interaction with bio-systems bring along concerns [22–24]. Therefore, new methodologies were developed to synthesize silver nanoparticles stabilized by certain agents by attaching their surface. Among these bio-molecules such as cysteine amino acid are gathering attention due to their availability and concurrent advantage of applicability to biological and sensing activities since this sulfur containing amino acid is a building molecule in macro and microorganisms [25, 26]. Therefore, the role of L-cysteine as a stabilization agent to prevent AgNPs from agglomeration can be a significant contribution to synthesis and application [27, 28].

This study reports a novel method for synthesis of stabilized L-CYS-AgNPs in aqueous acidic media. Reactions were carried out at ambient temperature without needing to heat source or other physical influences. This method is a concise, rapid, facile way of synthesizing cysteine capped, functionalized and stabilized AgNPs to hold for more than 2 months in colloid state.

## 2 Experimental

### 2.1 Materials

Silver nitrate ($AgNO_3$) was purchased from Merck, Darmstadt, Germany. L-Cysteine amino acid and other chemicals like sodium hydroxide ($NaBH_4$), methanol ($CH_3OH$) were provided by Daejung Chemicals & Materials Co., Ltd.

(Gyeonggi-do, South Korea). For all experimental work, solutions were prepared with de-ionized water. Beakers, test tubes, and other glasswares were rinsed three times with de-ionized water. Due to sensitivity of nanoparticles and synthesis process, all solutions and resulting dispersion were kept in dark to avoid any photochemical reaction at laboratory during experimental work.

### 2.2 Instrumentation

Water dispersible L-CYS-AgNPs in aqueous media were characterized by UV–Visible spectroscopy (UV–Vis) (UV-1800 Shimadzu, Japan) in the range of 300–700 nm. Transmission electron microscopy (TEM) (Philips CM12, FEI Ltd, UK) was attained at 80 kV. Energy dispersive spectroscopy (EDS) (Bruker X Flash 6060 EDS, California, USA) and Zeta potential analyzer (Malvern Instruments Ltd, serial number: MAL-1,135,362) were used for analysis of composition, size distribution and zeta potential.

### 2.3 Synthesis Process of L-Cysteine Capped Silver Nanoparticles

0.01 M stock solution of $AgNO_3$, 0.01 M solution of $NaBH_4$ and 0.5% stock solution of L-cysteine were prepared in proper volumetric flasks. All solutions have been prepared as aqueous solutions with de-ionized water. For the synthesis of AgNPs, 0.2 mL of silver nitrate solution was taken and used as a metal salt precursor, and added 0.05 mL of $NaBH_4$ as reducing agent to synthesize the nanoparticles. Mixture displayed yellow color immediately after addition of reducing agent and shaking by hand (Fig. 1). Following the reduction step, mixture was diluted to 10 and 0.08 mL of L-cysteine was added to the mixture for stabilization of prepared nanoparticles. Synthesis process was completed without heating and stirring at ambient temperature (Fig. 1). The resultant solution was analyzed by the using UV–Visible spectrometer was in the range of 300–700 nm at various times within 1–3 months in order to observe changes and resulting silver nanoparticles. The resulting (L-CYS-AgNPs) having
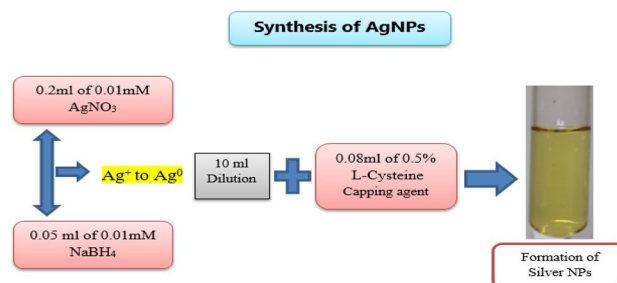


**Fig. 1** Scheme showing synthesis steps of L-cysteine stabilized silver nanoparticles

acidity (pH) of the reaction media has been 5.3, somewhat acidic, due to lacking base use and slightly acidic character of amino acid.

## 2.4 Procedure for Sample Preparation

### 2.4.1 Sample Preparation for AFM Analysis

L-CYS-AgNPs were dip coated for 35 s. on thin mica sheets then dried with nitrogen for 10 min. The AFM images for the coated AgNPs on mica sheet then recorded for analysis.

### 2.4.2 Sample Preparation for TEM

For the characterization of silver nanoparticles samples was drop cast on the surface of carbon coated copper grid and leave for air dried before analysis under the room temperature after dried the samples then TEM images were recorded.

### 2.4.3 Sample Preparation for Zeta Potential Analyzer

Zeta potential was performed on phase analysis light scattering (PALS) and used for having an insight into stability and size characteristics of nanoparticles. The instrument parameters were used for optimization such as wavelength, field frequency, voltage, electrical field, sample count rate and reference count rate. We have diluted a sample taken from the product mixture with 50 mL of double-distilled water. Then 0.02 mL of sodium chloride (NaCl) was applied to this as suspending electrolyte solution for the measurement of zeta potential. This mixture was shaken well for 30 min, and then zeta potential of silver nanoparticles was measured.

### 2.4.4 Sample Preparation for FTIR Analysis

FTIR study was carried out in Mid IR region within range of $500-4000\ cm^{-1}$. Large amount of silver nanoparticles solution was placed in petri dish and dried on a water bath set at 80 °C. Then dried material of nanoparticles was washed four times with methanol followed by de-ionized water. Furthermore, drying sample was kept in an oven for 30 min at 100 °C to complete evaporation of water molecule. The final product was scratched, collected and processed in KBr pellet for FTIR study using Bruker Tensor 27 spectrometer (Bruker, Bremen, Germany).

## 3 Results and Discussion

### 3.1 UV–Vis Analysis

For the synthesis of AgNPs using L-cysteine as stabilizing agent, AgNO$_3$ was first dissolved in Milli-Q water and free

silver ions (Ag$^+$) were released. By addition of highly reducing sodium borohydride into silver ion solution, free metallic silver (Ag$^0$) atoms were produced by the reduction of Ag$^+$ and they grew crystals into nanoparticles. Furthermore, L-cysteine was added into the mixture solution as a capping/stabilizing agent for preventing them from absorbing other particle or mixture components or attaching to each other's surface so as to avoid the agglomeration of nanoparticles. It is reported that when colloidal particles are smaller in size, they absorb and emit visible light with SPR activity [29]. Color for such AgNPs is expected to be yellow and SPR band would appear around 380–450 nm range. UV–Visible spectroscopy results confirmed that absorption spectra of our silver nanoparticles demonstrated consistent SPR band around 392 nm peak as shown in Fig. 2. Size of such nanoparticles would be less than 40 nm as indicated by TEM results provided in next sections. The electrostatic repulsion between AgNPs takes place with silver particles enclosed via molecules of L-CSY and caused by the negative charge is generated. Stability of synthesized silver nanoparticles was monitored and compared by UV–Visible spectroscopy on a monthly basis. Particles were stable and stored successfully without considerable changes for more than 3 months. Conformation of silver nanoparticles in aqueous solution was characterized by a single intense peak around 392 nm as shown in Fig. 2. The intensity of the band at this fixed wavelength of 392 nm was observed to decrease slightly as a function of time. Although intensity of absorbance weakens in time, wavelength remained constant and the relationship between time and absorbance showed linearity. All these findings support the stubborn stability of silver nanoparticles as shown in Fig. 3. An electrostatic repulsion takes place between AgNPs since nanoparticles are enclosed by molecules of L-cysteine. Since work function of silver atoms is among the highest (4.26–4.74 eV), they can bind electron rich sites strongly. This generation of cumulative negative charge throughout nanoparticle sphere, and this bestows an
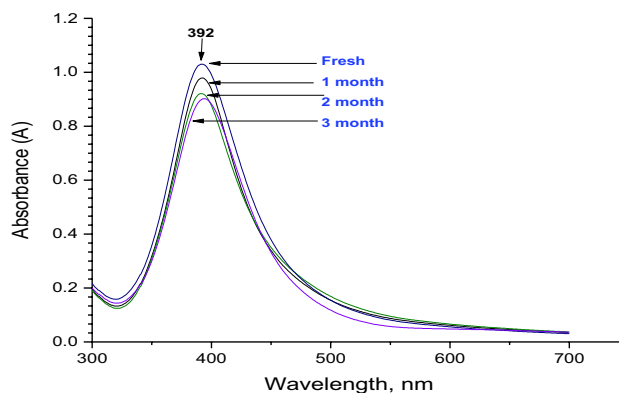
**Fig. 2** UV–Visible absorption spectra of L-cysteine stabilized silver nanoparticles from fresh to 3 month samples

$y = -0.0428x + 1.062$
$R^2 = 0.9696$
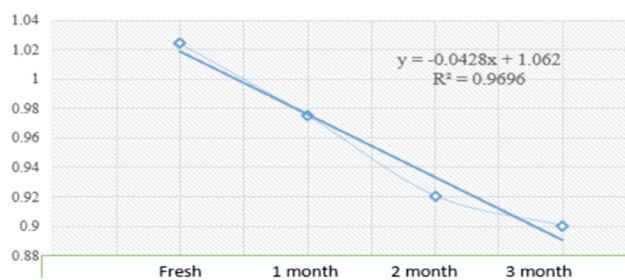
**Fig. 3** Almost linear relationship of decreasing absorbance of L-cysteine stabilized silver nanoparticles according to time

isolation nature and stability to nanoparticles. L-Cysteine has carboxylate, amine and thiol sites to act as legating absorbing grips.

## 3.2 AFM Analysis

AFM technique can be used to analyze size, geometry and distribution of nanomaterials. AgNPs were characterized by using atomic force microscopy for ascertaining details of size distribution and morphology. Topographical image of silver nanoparticles are shown in Fig. 4. AFM



**(a)**



**(b)**



**(c)**



**(d)**
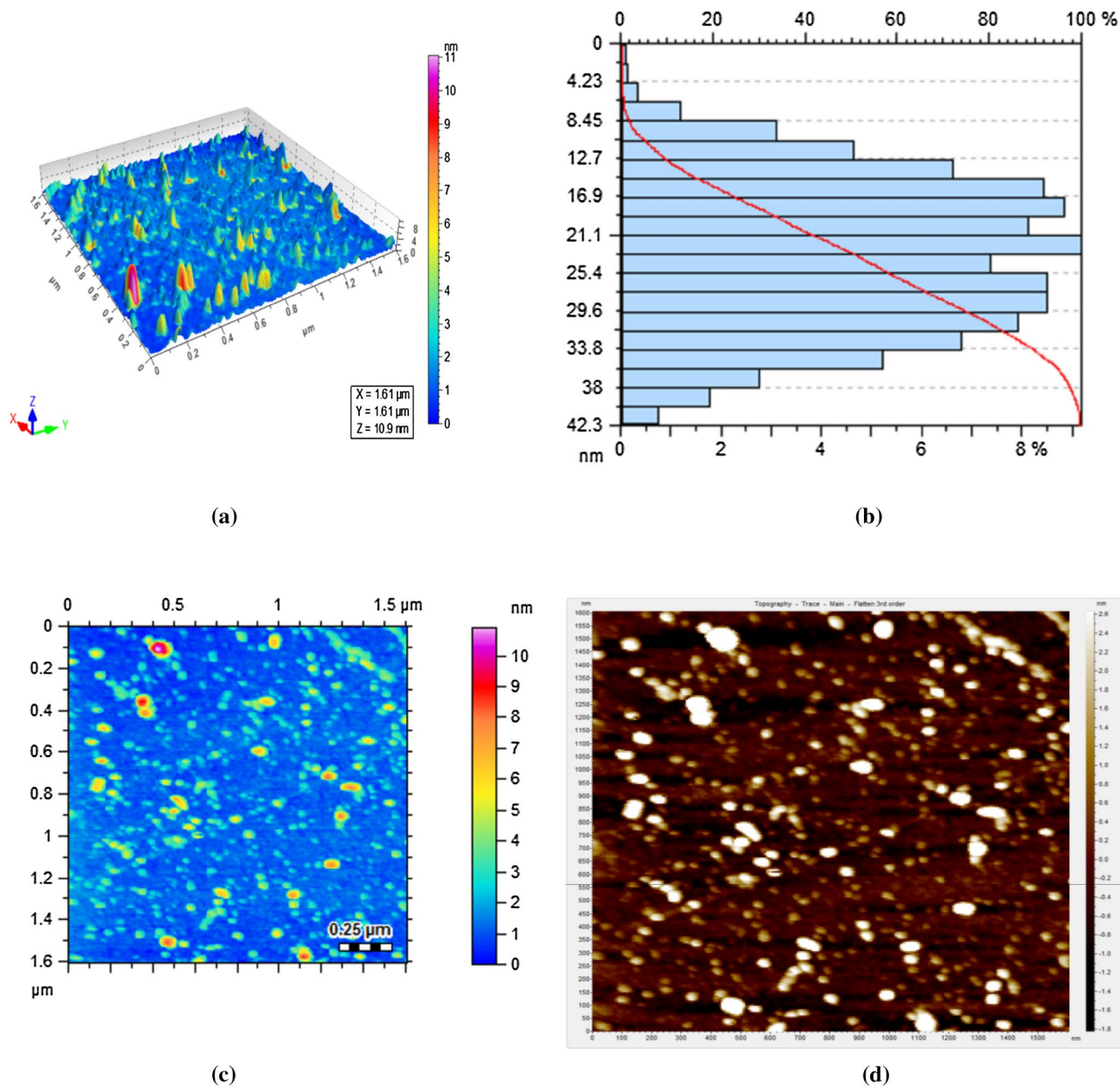
**Fig. 4** Topographical images of L-cysteine stabilized silver nanoparticles obtained by AFM **a** colored 3 D image, **b** size distribution histogram, **c** colored 2D image showing surface area covered by particles, **d** 3D surface topography
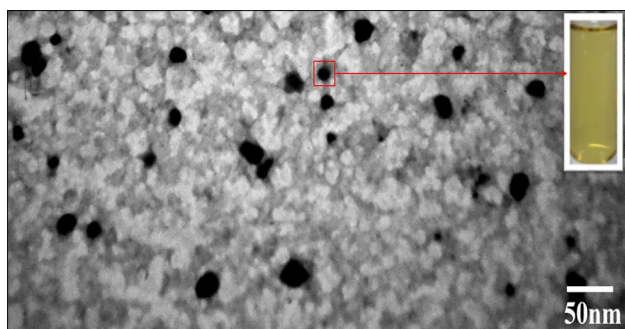
**Fig. 5** TEM image of spherical L-cysteine stabilized silver nanoparticles
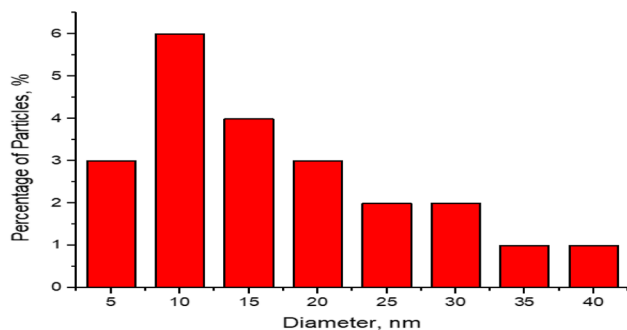


**Fig. 6** Histogram of size distribution of L-cysteine stabilized silver nanoparticles

characterization has been consistent with estimations drawn from the results of UV–Visible spectroscopy. Width and height of synthesized NPs were determined accordingly [30]. Measurement principle of an atomic force microscopy is customized to obtain data is commonly higher than data of x, y coordinates [31]. Particles are depicted in spherical shape and well dispersed on x, y plane. AFM results illustrated the profiles of nanoparticles in ranging sizes from 4 to 42 nm in height. The averages size has been around 21 nm.

### 3.3 TEM Analysis

Transmission electron microscopy (TEM) technique provides accurate information about size, geometry and morphology of AgNPs thorough neat images showing scaled diameter of the particles [32, 33]. Most of silver nanoparticles appeared to be in spherical shape and some had oval shape to some extent as shown in Fig. 5. Size of AgNPs ranged from 5 to 40 nm with an average size of 18 nm.

In previous research, TEM images suggested AgNPs to have diameters within 5–50 nm range and spherical geometry. Those were prepared by chemical reduction method using L-cysteine as a capping agent for the good use of their anti-bacterial and colorimetric sensing activities [34–36]. In another works, silver nanoparticles possessing sizes about

30–50 nm range were reported for their antibacterial activity against pathogens and bacteria [37, 38]. Sizes of nanoparticles set composing of a great deal of particles were measured by TEM in this work. A histogram was drawn to demonstrate the size distribution of the nanoparticles as shown in Fig. 6. Most of the particles were observed to have a size within 10–20 nm.

### 3.4 EDS Analysis

Energy dispersive spectroscopy technique is useful to gain an insight revealed into chemical composition and purity of nanostructures [39]. Vertical intensity and peak area related to the number of X-ray reflected or scattered by each atom of a specific type or its occupied shells which can be identified by the specific energy in (KeV) of the radiation belonging to that specific atom [40]. It has been revealed that elemental composition of silver nanoparticles was presented by a strong signal of silver atoms with 74.63% ratio, within the range of 3–4 keV [41]. Other researchers reported quantitative analysis of EDS for silver nanoparticles exhibiting 72.18% of silver content and similar stability performance [42]. Observation of carbon, sulfur, oxygen and nitrogen atoms on EDS graph is a sound evidence of L-cysteine capping on AgNPs even though ratios may not seem to very precise (Fig. 7). A more detailed analysis of X-ray photoelectron spectroscopy would show energy shifts on each atom (O, S, N) so as to clarify which atoms bind more strongly to Ag facets.

### 3.5 Zeta Potential Measurements

Analysis of zeta potential and particle size determination/distribution are important techniques of for AgNPs because other characterizations are also involved in investigation of physical stability, saturation, solubility and dissolution velocity etc. [43].

#### 3.5.1 Particles Size Analysis

Particle size and polydispersity indices of AgNPs in an aqueous dispersion were quantified instantly after the synthesis by the means of photon correlation spectroscopy. Sizes of AgNPs, were measured by granulometric method and recorded against particle number as described elsewhere [44]. Size of AgNPs ranged from 3 to 35 nm with an average size around at 23 nm by this method and rather deviated from TEM and AFM data as shown in Fig. 8. Particles size analysis showed that silver nanoparticles exhibit a polydispersity index (PDI) value of 0.40 and the intercept was 0.87 (Table 1).
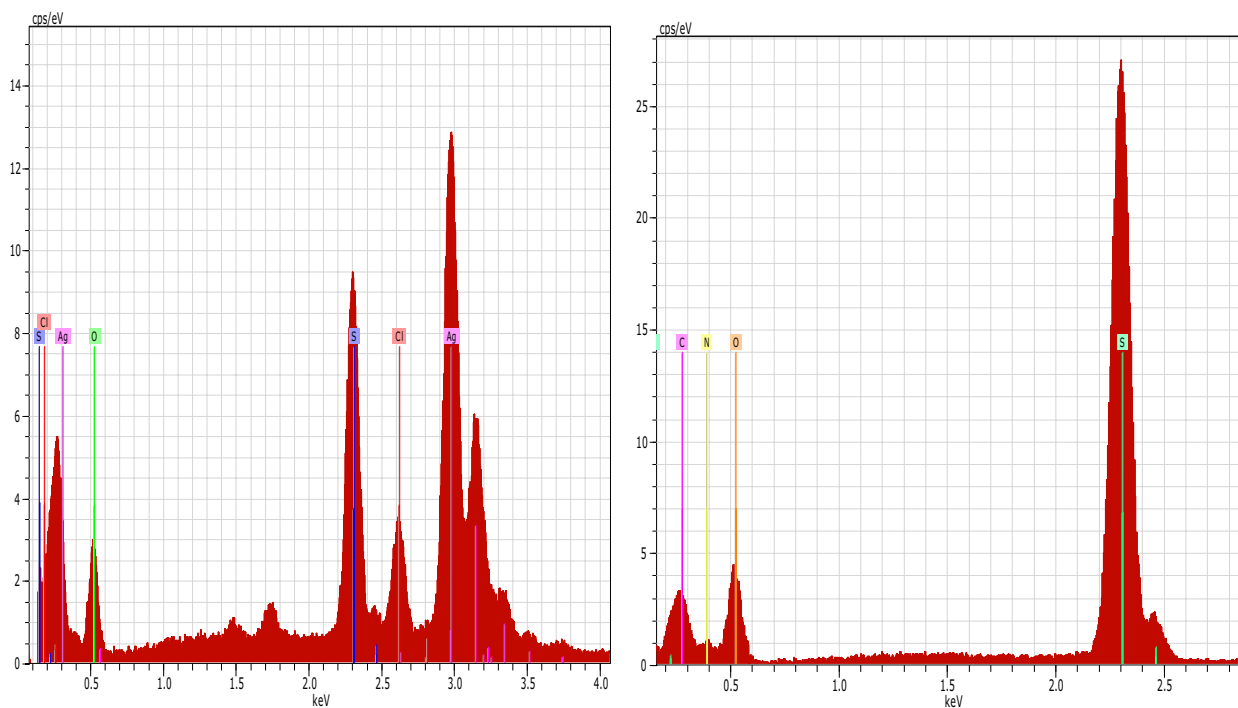
**(a)** `Spectrum: Acquisition`

| Element | Series | Unn. C [wt.%] | norm. C [wt.%] | Atom. C [at.%] | Error [%] |
|---------|--------|---------|---------|---------|------|
| Oxygen | K-series | 29.11 | 34.79 | 70.58 | 4.4 |
| Sulfur | K-series | 8.93 | 10.68 | 10.81 | 0.4 |
| Silver | L-series | 42.64 | 50.96 | 15.34 | 1.8 |
| Chlorine | K-series | 2.99 | 3.57 | 3.27 | 0.3 |
| | Total: | 83.68 | 100.00 | 100.00 | |

**(b)** `Spectrum: Acquisition`

| Element | Series | Unn. C [wt.%] | norm. C [wt.%] | Atom. C [at.%] | Error [%] |
|---------|--------|---------|---------|---------|------|
| Carbon | K-series | 14.31 | 12.74 | 18.05 | 2.1 |
| Nitrogen | K-series | 23.38 | 20.81 | 25.28 | 4.4 |
| Oxygen | K-series | 45.13 | 40.16 | 42.72 | 6.6 |
| Sulfur | K-series | 29.54 | 26.29 | 13.95 | 1.1 |
| | Total: | 112.36 | 100.00 | 100.00 | |

**Fig. 7** EDS graphs of **a** silver nanoparticles and **b** L-cysteine for elemental analysis
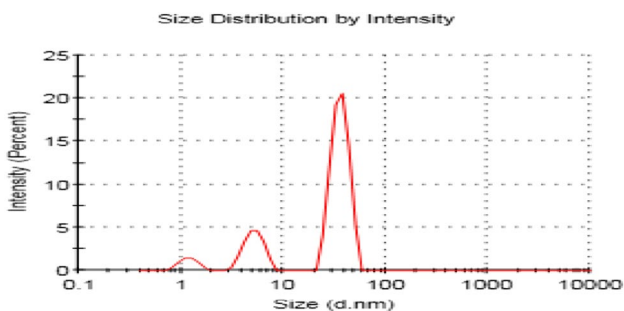


**Fig. 8** Percentage intensity of size distribution of silver nanoparticles

**Table 1** Mean particle size diameter, polydispersity indices of silver nanoparticles

| Peaks | Size (d nm) | Volume % | St. dev. (d nm) | |
|-------|-------------|----------|-----------------|---|
| Peak 1 | 32.51 | 0.0 | 6.970 | Z-average (d nm): 262.8 |
| Peak 2 | 4.644 | 4.3 | 1.093 | Pdi: 0.399 |
| Peak 3 | 1.103 | 95.7 | 0.2387 | Intercept: 0.870 |

### 3.5.2 Zeta Potential Analysis

A zeta potential characterization was used to analyze surface potential of AgNPs. Criterion for AgNPs to have high and low stability is about the magnitude of zeta potential being either higher than $+30$ mV or lower than $-30$ mV, and between these values, respectively [45]. It was reported that AgNPs possess a negative surface charge $-28.1$ mV along with a high surface charge and good stability [46]. The study suggested that consistent zeta potential value of 24.1 mV, is a highly negative potential value which is favorable for attainment of long term stability, high dispersity and good colloidal property of AgNPs because of negatives repulsion between nanoparticles [47]. Silver nanoparticles obtained in this work exhibited zeta potential of $+33.6$ mV positive charge and $-26.7$ mV of the negative charge of particles with a peak area of 100% intensity. These values show good stability of the AgNPs as shown in Fig. 9.

### 3.6 FTIR Analysis

Fourier transform infrared spectroscopy can be used to confirm that applied biomolecules are responsible for the reduction and capping of biosynthesized AgNPs, FTIR spectrum of L-cysteine capped AgNPs is shown in Fig. 10. Typical FTIR peaks for L-cysteine molecules can be distinctly seen on the spectrum. The FTIR peaks of L-cysteine can be categorized as follows: a weak carbonyl peak (C=O) stretching band around 1720 cm$^{-1}$, bending mode of amino group (–NH$_2$) at 1574 cm$^{-1}$ and its stretching band around 3500 cm$^{-1}$, C–H stretching band overlapped around 2940 cm$^{-1}$ and its bending bend around 1298, 1200, 1120, 1088 and 1036 cm$^{-1}$ absorptions can be associated with C–N, C–O, C–C and C–S stretching bands. Asymmetric and
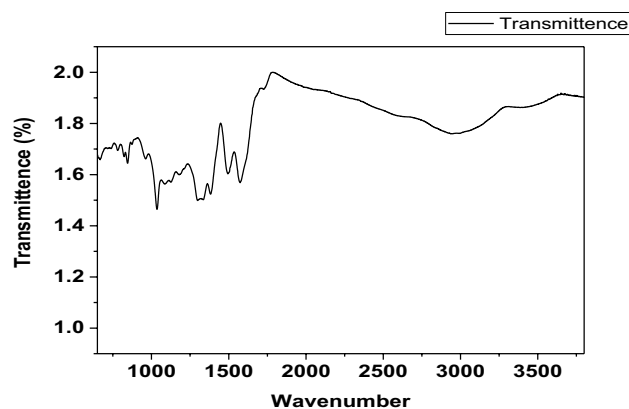
**Fig. 10** FTIR spectrum of L-cysteine stabilized silver nanoparticles

symmetric stretching of carboxylate group (COO$^{-1}$) can be attributed to 1382 and 1494 cm$^{-1}$, respectively. Therefore, these characteristics bands indicated the presence of cysteine on the surface of AgNPs, because a clear band of thiol group (–SH) was not observed in this spectrum. This is indicative of strong covalent (Ag–S) bonding denoted with peaks in low wave number region [48–51] as shown in Fig. 10.

## 4 Conclusions

This study summarizes a facile, eco-friendly, and one-pot rapid synthesis of water dispersible L-cysteine capped silver nanoparticles which can be stored for long periods as stable aqueous colloids. Synthesis process was fast and completed within a few minutes at room temperature without using a heating source and hazardous organic solvents. Images taken by AFM and TEM instruments

**Fig. 9** Zeta potential distribution of L-cysteine stabilized silver nanoparticles

**Results**

|  | Mean (mV) | Area (%) | St Dev (mV) |
|---|---|---|---|
| Zeta Potential (mV): -26.7 | Peak 1: -20.9 | 100.0 | 4.33 |
| Zeta Deviation (mV): 33.6 | Peak 2: 0.00 | 0.0 | 0.00 |
| Conductivity (m S/cm): 0.169 | Peak 3: 0.00 | 0.0 | 0.00 |
| Result quality : Good | | | |
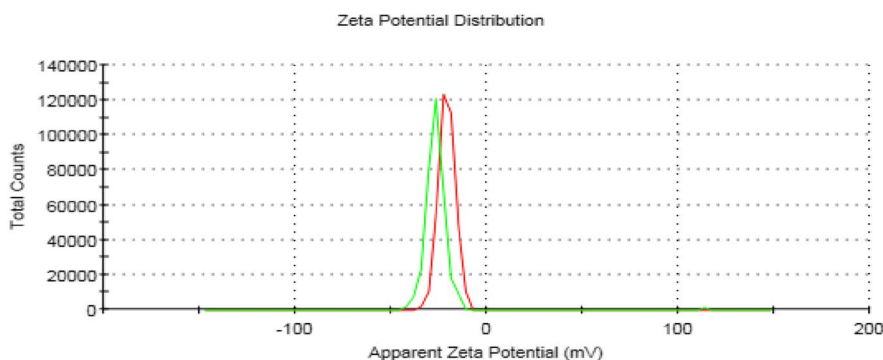
confirmed the formation of intended nanoparticles having an average size in the range of 18–21 nm in common. AgNPs existed mostly in spherical geometry and polydisperse form with sizes ranging from 5 to 40 nm. EDS revealed that chemical composition of AgNPs is composed of mainly Ag metal atoms and L-cysteine atoms (carbon, oxygen, sulfur etc.). FTIR spectroscopy revealed useful information about the surface interaction of functional groups of L-cysteine amino acid and AgNPs. Nanoparticles bear a net negative charge after being capped by L-cysteine molecules, which provides a strong stabilization for AgNPs and protection against agglomeration for long durations. These silver nanoparticles would be benefitted highly for catalysis and sensing applications.

# References

1. J. Pranay, A. Vibhor, Int. J. Nano Mater. Sci. **1**, 108 (2012)
2. S. Esir, Y. Junejo, A. Baykal, M. Toprak, H. Sozeri, J. Inorg. Organomet. Polym. Mater. **24**, 722 (2014)
3. Y. Junejo, A. Baykal, J. Sirauddin, Inorg. Organomet. Polym. Mater. **24**, 401 (2014)
4. F. Zhang, Y. Sun, D. Tian, W.S. Shin, J.S. Kim, H. Li, Chem. Commun. **52**, 12685 (2016)
5. K. Sudhakar, S.J. Moloi, K.M. Rao, J. Inorg. Organomet. Polym. Mater. **27**, 1450 (2017)
6. S.S. Hassan, S. Panhwar, A. Nafady, A.M. Al-Enizi, Sirajuddin, S.T.H. Sherazi, M.S. Kalhoro, M. Arain, M.R. Shah, M.Y. Talpur, J. Electrochem. Soc. **164**, 427 (2017)
7. S. Dhar, P. Murawala, A. Shiras, V. Pokharkar, B. Prasad, Nanoscale **4**, 563 (2012)
8. S. Gurunathan, J.H. Park, J.W. Han, J.H. Kim, Int. J. Nanomed. **10**, 4203 (2015)
9. M. Tudose, D.C. Culita, A.M. Musuc, G. Marinescu, S. Somacescu, C. Munteanu, C. Bleotu, M.C. Chifiriuc, J. Inorg. Organomet. Polym. Mater. **26**, 1043 (2016)
10. Y.A. Krutyakov, A.A. Kudrinskiy, A.Y. Olenin, G.V. Lisichkin, Russ. Chem. Rev. **77**, 233 (2008)
11. R. Singh, U.U. Shedbalkar, S.A. Wadhwani, B.A. Chopade, Appl. Microbiol. Biotechnol. **99**, 4579 (2015)
12. S. Agnihotri, S. Mukherjia, S. Mukherji, Nanoscale **5**, 7328 (2013)
13. C. Ignác, Nanostruct. Sci. Technol. **1**, 554 (2017)
14. S. Agnihotri, S. Mukherjia, S. Mukherji, Appl. Nanosci. **2**, 179 (2012)
15. D. Steinigeweg, S. Schlücker, Chem. Commun. **48**, 8682 (2012)
16. Y. Liu, J. Tan, A. Thomas, D. Ou-Yang, V.R. Muzykantov, Res. Pharm. Sci. **3**, 181 (2014)
17. U. Hansen, A.F. Thünemann, Langmuir **31**, 6842 (2015)
18. K. Logaranjan, A.J. Raiza, S.C.B. Gopinath, Y. Chen, K. Pandian, Nanoscale Res. Lett. **11**, 520 (2016)
19. S. Agnihotri, S. Mukherji, S. Mukherji, RSC Adv. **4**, 3974 (2014)
20. S. Kalathil, J. Lee, M.H. Cho, Green Chem. **13**, 1482 (2011)
21. A.A. El-Kheshen, S.F.G. El-Rab, Pharm. Chem. **4**, 53 (2012)
22. S. Rajeshkumar, L.V. Bharath, Chem. Biol. Interact. **273**, 219 (2017)
23. M. Chauhan, C. Feizullayeva, K. Melepura, S. Matam, A. Patel, Q. Johnson, B.P.S. Chauhan, J. Inorg. Organomet. Polym. Mater. **24**, 994 (2014)
24. S.E. Kudaibergenov, G.S. Tatykhanova, B.S. Selenova, J. Inorg. Organomet. Polym. Mater. **26**, 1198 (2016)
25. Q.H. Tran, V.Q. Nguyen, A.T. Le, Adv. Nat. Sci.: Nanosci. Nanotechnol. **4**, 033001 (2013)
26. W. Zhang, L. Zhang, Y. Sun, Front. Chem. Sci. Eng. **9**, 494 (2015)
27. R.S. Patil, M.R. Kokate, S.S. Kolekar, Spectrochim. Acta Part A **91**, 234 (2012)
28. P.V. Dong, C.H. HaLe, T.B. Kasbohm, Inter. Nano Lett. **2**, 1 (2012)
29. G.A. Eiceman, M.R. Salazar, M.R. Rodriguez, T.F. Limero, S.W. Beck, J.H. Cross, R. Young, J.T. James, Anal. Chem. **65**, 1696 (2013)
30. K.H. Sodha, J.K. Jadav, Int. J. Pharma Bio Sci. **6**, 199 (2015)
31. J.E. Andrade, R. Machado, Polímeros **23**, 19 (2013)
32. D. Chicea, Rom. Rep. Phys. **66**, 778 (2014)
33. D. Peddis, G. Muscas, R. Mathieu, P. Anil Kumar, G. Varvaro, G. Singh, I. Orue, D. Gil-Carton, L. Marcano, A. Muela, M.L. Fdez-Gubieda, Faraday Discuss. **191**, 177 (2016)
34. M.M. Khan, S. Kalathil, Bull. Korean Chem. Soc. **33**, 2592 (2012)
35. K. Chandraker, R. Nagwanshi, S.K. Jadhav, K.K. Ghosh, M.L. Satnami, Spectrochim. Acta Part A **181**, 47 (2017)
36. S. Babu, O. Michelle, K. Claville, Ghebreyessus, J. Exp. Nanosci. **16**, 1242 (2015)
37. K.V. Selvi, T. Sivakumar, Int. J. Curr. Microbiol. Appl. Sci. **1**, 56 (2012)
38. F. Kang, D. Zhu, J. Environ. Qual. **42**, 1441 (2013)
39. Y. Liu, Z. Zheng, J.N. Zara, C. Hsu, D.E. Soofer, K.S. Lee, R.K. Siu, L.S. Miller, X. Zhang, D. Carpenter, C. Wang, K. Ting, C. Soo, Biomaterials **33**, 8745 (2012)
40. C. Jayaseelan, A.A. Rahuman, Parasitol. Res. **111**, 1369 (2012)
41. P. Jegadeeswaran, R. Shivaraj, R. Venckateshagreen, Dig. J. Nanomater. Biostruct. **7**, 991 (2012)
42. S. Saha, J. Sarkar, D. Chattopadhyay, S. Patra, Dig. J. Nanomater. Biostruct. **5**, 887 (2011)
43. V. Kaushik, S.C. Joshi, Asian J. Pharm. Clin. Res. **8**, 179 (2015)
44. D. Sivaraman, P. Panneerselvam, P. Muralidharan, T.P. Prabhu, R.V. Kumar, Int. J. Sci. Eng. Res. **4**, 2280 (2013)
45. J. Firehouse, M. Lalitha, Der Pharma Chemica **24**, 2320 (2012)
46. J. Mohammed, H. Mohammed, Int. J. Sci. Eng. Res. **5**, 381 (2014)
47. P. Bobbu, V.R. Netala, S. Aishwarya, I. Rama, M. Reddy, V.S. Kotakadi, V. Tartte, Int. J. Pharm. Pharm. Sci. **8**, 341 (2016)
48. S. Mukherjee, D. Chowdhury, R. Kotcherlakota, Theranostics **4**, 316 (2014)
49. R.A. Soomro, A. Nafady, Sirajuddin, N. Memon, S.T.H. Sherazi, Talanta **130**, 415 (2014)
50. N.H. Kalwar, A. Nafady, S.S.T.H. Sherazi, R.A. Soomro, K.R. Hallam, A.R. Khaskheli, A.A. Jamali, Mater. Exp. **5**, 121 (2015)
51. S. Pandey, G.K. Goswami, K.K. Nanda. Int. J. Biol. Macromol. **51**, 583 (2012)